# Series of Ag(I) Coordination Complexes Derived from Aminopyrimidyl Ligands and Dicarboxylates: Syntheses, Crystal Structures, and Properties

Di Sun, Na Zhang, Rong-Bin Huang,* and Lan-Sun Zheng

*State Key Laboratory of Physical Chemistry of Solid Surface, Department of Chemistry, College of Chemistry and Chemical Engineering, Xiamen University, Xiamen 361005, China*

**ABSTRACT:** A series of new metal−organic frameworks, namely, $[Ag(mapym)(suc)_{0.5} \cdot 0.5H_2O]_n$ (**1**), $[Ag_2(mapym)_2(glu) \cdot 1.5H_2O]_n$ (**2**), $[Ag_2(mapym)_2(ipa) \cdot 2H_2O]_n$ (**3**), $[Ag_2(mapym)_2(tpa)(H_2O)]_n$ (**4**), $[Ag(dmapym)_2(ox)_{0.5} \cdot H_2O]$ (**5**), and $[Ag(dmapym)(bbdc)_{0.5} \cdot 0.5H_2O]_n$ (**6**) (mapym = 2-amino-4-methylpyrimidine, dmapym = 2-amino-4,6-dimethylpyrimidine, $H_2suc$ = succinic acid, $H_2glu$ = glutaric acid, $H_2ipa$ = isophthalic acid, $H_2tpa$ = terephthalic acid, $H_2ox$ = oxalic acid, $H_2bbdc$ = 4,4-bibenzenedicarboxylic acid), have been synthesized and structurally characterized. Complexes **1** and **2** exhibit two-dimensional (2D) interpenetrated and double-sheet structures, respectively. Complex **3** is a three-dimensional (3D) framework constructed through unusual 2D → 3D parallel interpenetration of a corrugated 2D $4^4$-sql net. Complex **5** is a 0-dimensional (0D) H-shaped molecule, and the self-complementary N−H···N hydrogen bonds incorporating $R_4^4(14)$ hydrogen bond motifs extend these molecules into a 3D supramolecular framework. Complexes **4** and **6** are also 2D sheets constructed with a similar fashion to that of **1** and **2** but with aryl-dicarboxylate as bridge. The results show that the coordination geometry of the Ag(I) ions and the configuration and coordination mode of dicarboxylates as well as the competition between steric and electronic effects of methyl groups on aminopyrimidyl ligands play crucial roles in determining the structure of the complexes. Additionally, results about IR spectra, thermogravimetric curves, and photoluminescence spectra were addressed.
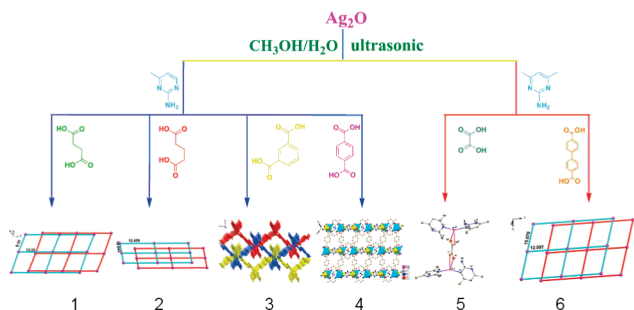
## Introduction

Over the past two decades, the crystal engineering of coordination complexes (CCs) has provoked unparalleled attention and imagination within coordination chemistry based on assembly of judiciously chosen metal ions ( joints) and multifunctional organic ligands (struts). Much effort has been devoted to controlling the structures of CCs because their intriguing properties and potential applications are strongly dependent on their structures.[1] Despite some recent advancement, the ability to predict and control the supramolecular assembly remains a longstanding challenge, and much more elaborate and systematic work is required to comprehend the inter- and intramolecular forces that determine the fashions of molecular structure and crystal packing in the solid state. A better understanding of the influence factors of structure, including inbeing of the metal ions and the predesigned organic ligands[2] as well other factors such as the medium,[3] the pH value of the solution,[4] the temperature,[5] the counterion with different bulk or coordination ability, the template, and the metal/ligand ratio,[6] is a prerequisite to rationally design, predict, and synthesize CCs functional materials. Including the above-mentioned factors, the noncovalent forces, such as hydrogen-bonding, $\pi$···$\pi$ stacking, metal···metal interactions based on $d^{10}$ metal cations, and metal···$\pi$, C−H···$\pi$, and anion···$\pi$ interactions, also intensively impact the supramolecular topology and dimensionality.[7] In contrast to other transition metal ions, Ag(I) ion, with a $d^{10}$ closed-shell electronic configuration, is very enthralling, as it shows (i) a dynamic range of coordinative geometries, including linear, trigonal-planar, tetrahedral, and trigonal-pyramidal, with occasional instances of square-planar, pyramidal, and octahedral geometry,[8] and (ii) a tendency to form an argentophilic interaction,[9] both of which

may lead to discovery of novel structural motifs. These contain high-nuclearity silver chalcogenide clusters,[10] one-dimensional chains, which can be single-, double-, and triple-stranded helix,[11] two-dimensional sheets with a variety of connectivities such as $4^4$-sql and $6^3$-hcb nets,[12] and three-dimensional structures, such as diamondoid and chiral adamantoid network.[13] Such compounds can also exhibit other appealing structural phenomena from simple guest inclusion[14] to interpenetration (0D → 3D, 1D → 2D, 2D → 2D, and 2D → 3D)[15] and even polycatenanes.[16] Organic ligands with carboxylic groups are of especial interest and have been widely used to construct various CCs, owing to their fascinating characteristics, including strong coordination ability, diverse coordination modes, different organic skeletons of carboxylate linkers, and abundant hydrogen-bonding and aromatic stacking interactions.[17] In particular, the different orientations of carboxylic groups situated in the organic skeletons may link metal ions in different directions and distances into extended networks.[18−20] On the other hand, amino-containing heterocyclic N-donor ligands, such as 2-aminopyridine, are versatile ligands because of documented metal binding patterns including the ring nitrogen atom[21] or the exocyclic amino group,[22] occasionally in equilibrium,[23] and simultaneously both positions, in either a chelating or bridging fashion.[24] Moreover, the stereochemically associative amino group also demonstrated the ability to form very stable hydrogen-bonded arrays.[25]

Taking into account the points aforementioned and considering our previous work,[26] we continue to focus on the reactions of closed-shell $d^{10}$ Ag(I) with dipodal amino-pyrimidyl and auxiliary dicarboxylate ligands and investigate the influence of dicarboxylate and substituent on the structure of the resultant complexes as well as their properties. In this paper, we report the syntheses, crystal structures, and properties of six new mixed-ligand coordination complexes, namely, $[Ag(mapym)(suc)_{0.5} \cdot 0.5H_2O]_n$ (**1**),

---

*To whom correspondence should be addressed. E-mail: rbhuang@xmu.edu.cn. Fax: 86-592-2183074.

**Scheme 1. Preparation Route of Ag(I) Mixed-Ligand Coordination Complexes from the N-Donor and O-Donor Ligands**



$[Ag_2(mapym)_2(glu)\cdot1.5H_2O]_n$ (**2**), $[Ag_2(mapym)_2(ipa)\cdot2H_2O]_n$ (**3**), $[Ag_2(mapym)_2(tpa)(H_2O)]_n$ (**4**), $[Ag(dmapym)_2(ox)_{0.5}\cdot H_2O]$ (**5**), and $[Ag(dmapym)(bbdc)_{0.5}\cdot0.5H_2O]_n$ (**6**) (mapym = 2-amino-4-methylpyrimidine, dmapym = 2-amino-4,6-dimethylpyrimidine, $H_2suc$ = succinic acid, $H_2glu$ = glutaric acid, $H_2ipa$ = isophthalic acid, $H_2tpa$ = terephthalic acid, $H_2ox$ = oxalic acid, $H_2bbdc$ = 4,4-bibenzenedicarboxylic acid) (Scheme 1).

## Experimental Section

**Materials and General Methods.** All chemicals and solvents used in the syntheses were of analytical grade and used without further purification. IR spectra were measured on a Nicolet 740 FTIR spectrometer in the range $4000-400$ cm$^{-1}$. Elemental analyses were carried out on a CE instruments EA 1110 elemental analyzer. Photoluminescence spectra were measured on a Hitachi F-4500 fluorescence spectrophotometer (slit width, 2.5 nm; sensitivity, high). TG curves were measured from 25 to 800 °C on a SDT Q600 instrument at the heating rate 5 °C/min under a N$_2$ atmosphere (100 mL/min). X-ray powder diffractions were measured on a Panalytical X-Pert pro diffractometer with Cu Kα radiation.

**Preparation of Complex 1−6. [Ag(mapym)(suc)$_{0.5}\cdot$0.5H$_2$O]$_n$ (1).** Ag$_2$O (116 mg, 0.5 mmol), mapym (109 mg, 1 mmol), and H$_2$suc (118 mg, 1 mmol) were reacted in methanol/H$_2$O media (15 mL, v/v = 2:1) in the presence of ammonia (0.5 mL) under ultrasonic treatment (160 W, 40 kHz, 50 °C). The resultant colorless solution was allowed to slowly evaporate under a 38 °C constant environment for one week to give colorless crystals of **1**. The crystals were isolated by filtration and washed with deionized water and dried in air. Yield: *ca.* 82% based on Ag$_2$O. Elemental analysis: Anal. Calc for Ag$_2$C$_{14}$H$_{20}$N$_6$O$_5$: C, 29.60; H, 3.55; N, 14.79. Found: C, 29.55; H, 3.62; N, 14.88. Selected IR peaks (cm$^{-1}$): 3412 (s), 3331 (s), 3175 (s), 2926 (w), 1663 (s), 1576 (s), 1482 (s), 1396 (m), 1222 (w), 801 (w), 653 (s), 557 (w).

**[Ag$_2$(mapym)$_2$(glu)$\cdot$1.5H$_2$O]$_n$ (2).** Synthesis of **2** was similar to that of **1**, but with H$_2$glu (132 mg, 1 mmol) instead of H$_2$suc. Colorless crystals of **2** were obtained in 68% yield based on Ag$_2$O. Elemental analysis: Anal. Calc For Ag$_4$C$_{30}$H$_{46}$N$_{12}$O$_{11}$: C, 30.48; H, 3.92; N, 14.22. Found: C, 30.51; H, 4.00; N, 14.18. Selected IR peaks (cm$^{-1}$): 3418 (s), 3325 (s), 3163 (s), 2957 (w), 1658 (s), 1579 (s), 1482 (m), 1400 (m), 1345 (w), 1218 (w), 848 (w), 794 (w), 554 (w).

**[Ag$_2$(mapym)$_2$(ipa)$\cdot$2H$_2$O]$_n$ (3).** Synthesis of **3** was similar to that of **1**, but with H$_2$ipa (166 mg, 1 mmol) instead of H$_2$suc. Colorless crystals of **3** were obtained in 57% yield based on Ag$_2$O. Elemental analysis: Anal. Calc for Ag$_2$C$_{18}$H$_{22}$N$_6$O$_6$: C, 34.09; H, 3.50; N, 13.25. Found: C, 34.13; H, 3.46; N, 13.22. Selected IR peaks (cm$^{-1}$): 3406 (s), 3318 (s), 3157 (s), 1657 (s), 1608 (s), 1591 (s), 1596 (s), 1479 (s), 1377 (m), 1223 (w), 732 (w), 554 (w), 506 (w).

**[Ag$_2$(mapym)$_2$(tpa)(H$_2$O)]$_n$ (4).** Synthesis of **4** was similar to that of **1**, but with H$_2$tpa (166 mg, 1 mmol) instead of H$_2$suc. Colorless crystals of **4** were obtained in 77% yield based on Ag$_2$O. Elemental analysis: Anal. Calc for Ag$_2$C$_{18}$H$_{20}$N$_6$O$_5$: C, 35.09; H, 3.27; N, 13.64. Found: C, 35.14; H, 3.36; N, 13.58. Selected IR peaks (cm$^{-1}$): 3412 (s), 3325 (s), 3163 (s), 1659 (s), 1574 (s), 1481 (s), 1384 (s), 1217 (m), 1015 (w), 820 (w), 749 (w), 508 (w).

**[Ag(dmapym)$_2$(ox)$_{0.5}\cdot$H$_2$O] (5).** Ag$_2$O (116 mg, 0.5 mmol), dmapym (123 mg, 1 mmol) and H$_2$ox$\cdot$2H$_2$O (126 mg, 1 mmol) in methanol/H$_2$O media (15 mL, v/v = 2:1) were reacted in the presence of ammonia (0.5 mL) under ultrasonic treatment (160 W, 40 kHz, 50 °C). Colorless crystals of **5** were obtained in 65% yield based on Ag$_2$O. Elemental analysis: Anal. Calc for Ag$_2$C$_{26}$H$_{40}$N$_{12}$O$_6$: C, 37.52; H, 4.84; N, 20.19. Found: C, 37.49; H, 4.90; N, 20.24. Selected IR peaks (cm$^{-1}$): 3425 (s), 3398 (s), 3309 (s), 3129 (s), 2918 (w), 1665 (m), 1600 (s), 1470 (m), 1391 (m), 1310 (m), 1235 (w), 795 (w), 773 (w), 629 (w).

**[Ag(dmapym)(bbdc)$_{0.5}\cdot$0.5H$_2$O]$_n$ (6).** Synthesis of **6** was similar to that of **5**, but with H$_2$bbdc (242 mg, 1 mmol) instead of H$_2$ox$\cdot$2H$_2$O. Colorless crystals of **6** were obtained in 65% yield based on Ag$_2$O. Elemental analysis: Anal. Calc for Ag$_2$C$_{26}$H$_{28}$N$_6$O$_5$: C, 43.36; H, 3.92; N, 11.67. Found: C, 43.34; H, 3.99; N, 11.72. Selected IR peaks (cm$^{-1}$): 3400 (s), 3312 (m), 3144 (m), 1590 (s), 1541 (s), 1466 (w), 1393 (s), 1229 (w), 834 (w), 765 (w).

**X-ray Crystallography.** Single crystals of complexes **1−6** with appropriate dimensions were chosen under an optical microscope and quickly coated with high vacuum grease (Dow Corning Corporation) before being mounted on a glass fiber for data collection. Data were collected on a Rigaku R-AXIS RAPID Image Plate single-crystal diffractometer with a graphite-monochromated Mo Kα radiation source (λ = 0.71073 Å) operating at 50 kV and 90 mA in ω scan mode for **1−6**. A total of 44 × 5.00° oscillation images was collected, each being exposed for 5.0 min. Absorption correction was applied by correction of symmetry-equivalent reflections using the ABSCOR program.[27] In all cases, the highest possible space group was chosen. All structures were solved by direct methods using SHELXS-97[28] and refined on $F^2$ by full-matrix least-squares procedures with SHELXL-97.[29] Atoms were located from iterative examination of difference $F$-maps following least-squares refinements of the earlier models. Hydrogen atoms were placed in calculated positions and included as riding atoms with isotropic displacement parameters $1.2-1.5$ times $U_{eq}$ of the attached C or N atoms. The hydrogen atoms attached to oxygen were refined with $O-H = 0.85$ Å and $U_{iso}(H) = 1.2U_{eq}(O)$. All structures were examined using the Addsym subroutine of PLATON[30] to ensure that no additional symmetry could be applied to the models. Pertinent crystallographic data collection and refinement parameters are collated in Table 1. Selected bond lengths and angles for **1−6** are collated in Table 2. The hydrogen bond geometries for **1−6** are shown in Table S1 (Supporting Information).

## Result and Discussion

**Synthesis.** The syntheses of complexes **1−6** were carried out in the darkness to avoid photodecomposition, and they are summarized in Scheme 1. The formation of the products is not significantly affected by changes of the reaction mole ratio of organic ligands to metal ions. As is well-known, the reactions of Ag(I) with dicarboxylates in aqueous solution often result in the formation of insoluble silver salts, presumably due to the fast coordination of the carboxylates to Ag(I) ions to form polymers.[31] Hence, properly lowering the reaction speed, such as using ammoniacal conditions or the layer-separation diffusion method, may favor the formation of crystalline products.[32] Ag$_2$O was used instead of AgNO$_3$ or other common Ag(I) salts in order to promote the carboxylates instead of small anions to coordinate to the Ag(I) centers. The ultrasonic method has found an important niche in the preparation of inorganic materials.[33] The high local temperatures and pressures, combined with extraordinarily rapid cooling, provide a unique means for driving chemical reactions under extreme conditions. In this system, the ultrasound technique also realizes the rapid (10 min) and efficient (maximum thirty different experiments in one batch) preparation of CCs.

**Structure Descriptions. [Ag(mapym)(suc)$_{0.5}\cdot$0.5H$_2$O]$_n$ (1).** Single-crystal X-ray diffraction analysis reveals that complex **1** represents a 2D polymeric structure with irregular quadrilateral grids which crystallizes in the space group $P2/c$.

**Table 1. Crystal Data for 1–6[a]**

| compd | 1 | 2 | 3 | 4 | 5 | 6 |
|---|---|---|---|---|---|---|
| empirical formula | $Ag_2C_{14}H_{20}N_6O_5$ | $Ag_4C_{30}H_{46}N_{12}O_{11}$ | $Ag_2C_{18}H_{22}N_6O_6$ | $Ag_2C_{18}H_{20}N_6O_5$ | $Ag_2C_{26}H_{40}N_{12}O_6$ | $Ag_2C_{26}H_{28}N_6O_5$ |
| formula wt | 568.10 | 1182.27 | 634.16 | 616.14 | 832.44 | 720.28 |
| crystal system | monoclinic | triclinic | monoclinic | triclinic | triclinic | monoclinic |
| space group | $P2/c$ | $P\bar{1}$ | $P2_1/c$ | $P\bar{1}$ | $P\bar{1}$ | $C2/c$ |
| $a$ (Å) | 9.4815(19) | 9.0313(11) | 11.742(4) | 8.9879(13) | 7.122(2) | 15.676(3) |
| $b$ (Å) | 8.6468(18) | 10.0434(13) | 10.703(4) | 11.2940(18) | 10.418(4) | 15.049(3) |
| $c$ (Å) | 12.217(3) | 12.4591(16) | 18.894(6) | 12.2234(17) | 11.812(4) | 12.097(2) |
| $\alpha$ (deg) | 90 | 97.387(7) | 90 | 111.792(14) | 66.138(6) | 90 |
| $\beta$ (deg) | 110.667(3) | 109.497(3) | 110.545(18) | 98.424(12) | 86.572(8)) | 107.31(3) |
| $\gamma$ (deg) | 90 | 101.338(6) | 90 | 109.836(14) | 88.632(7) | 90 |
| $V$ (Å$^3$) | 937.2(3) | 1021.2(2) | 2223.5(13) | 1029.7(3) | 800.1(5) | 2040.04(9) |
| $T$ (K) | 298(2) | 298(2) | 298(2) | 298(2) | 298(2) | 298(2) |
| $Z$, $D_{calcd}$ (Mg/m$^3$) | 2, 2.013 | 1, 1.922 | 4, 1.894 | 2, 1.987 | 1, 1.728 | 4, 1.756 |
| $F(000)$ | 560 | 586 | 1256 | 608 | 422 | 1440 |
| $\mu$ (mm$^{-1}$) | 2.128 | 1.959 | 1.809 | 1.946 | 1.284 | 1.485 |
| refl. collected/unique | 4509/1640 | 8053/3574 | 10704/3841 | 9059/3993 | 3390/2657 | 8899/2383 |
| $R_{int}$ | 0.0226 | 0.0367 | 0.0410 | 0.0602 | 0.0189 | 0.0388 |
| parameters | 125 | 264 | 291 | 281 | 212 | 184 |
| final $R$ indices [$I > 2\sigma(I)$] | $R_1 = 0.0291$ | $R_1 = 0.0399$ | $R_1 = 0.0732$ | $R_1 = 0.0389$ | $R_1 = 0.0457$ | $R_1 = 0.0288$ |
| | $wR_2 = 0.0655$ | $wR_2 = 0.1048$ | $wR_2 = 0.1561$ | $wR_2 = 0.0641$ | $wR_2 = 0.1341$ | $wR_2 = 0.0621$ |
| $R$ indices (all data) | $R_1 = 0.0311$ | $R_1 = 0.0461$ | $R_1 = 0.0854$ | $R_1 = 0.0766$ | $R_1 = 0.0496$ | $R_1 = 0.0397$ |
| | $wR_2 = 0.0665$ | $wR_2 = 0.1108$ | $wR_2 = 0.1622$ | $wR_2 = 0.0702$ | $wR_2 = 0.1358$ | $wR_2 = 0.0680$ |
| max./ min., $\Delta\rho$ (e·Å$^{-3}$) | 0.829/−0.320 | 1.289/−0.834 | 1.410/−1.338 | 0.566/−0.541 | 1.532/−0.666 | 0.456/−0.441 |

[a] $R_1 = \sum ||F_o| - |F_c||/\sum |F_o|$; $wR_2 = [\sum w(F_o^2 - F_c^2)^2]/\sum w(F_o^2)^2]^{1/2}$.

**Table 2. Selected Bond Lengths (Å) and Angles (deg) for 1–6[a]**

Complex **1**

| | | | | | | | |
|---|---|---|---|---|---|---|---|
| Ag1−O2$^i$ | 2.240(2) | Ag1···Ag2 | 3.0645(9) | Ag2−N3$^i$ | 2.167(3) | Ag1−N2$^{ii}$ | 2.453(3) |
| O2$^i$−Ag1−O2 | 166.50(15) | N2$^{ii}$−Ag1−N2$^{iii}$ | 111.23(15) | O2$^i$−Ag1−N2$^{iii}$ | 91.45(10) | N3$^i$−Ag2−N3 | 170.49(16) |

Complex **2**

| | | | | | | | |
|---|---|---|---|---|---|---|---|
| Ag1−N2 | 2.236(3) | Ag1···Ag2 | 3.1284(7) | Ag2−N3$^{ii}$ | 2.206(4) | Ag2−O1 | 2.566(4) |
| Ag1−O3$^i$ | 2.298(3) | Ag1−N6 | 2.477(4) | Ag2−N5$^{iii}$ | 2.208(4) | Ag1−O2 | 2.378(4) |
| N2−Ag1−O3$^i$ | 144.05(12) | O2−Ag1−N6 | 96.70(14) | N3$^{ii}$−Ag2−O1 | 103.22(13) | N3$^{ii}$−Ag2−N5$^{iii}$ | 152.32(13) |
| N2−Ag1−O2 | 99.90(14) | O3$^i$−Ag1−N6 | 80.73(12) | N2−Ag1−N6 | 120.08(13) | N5$^{iii}$−Ag2−O1 | 97.06(15) |

Complex **3**

| | | | | | | | |
|---|---|---|---|---|---|---|---|
| Ag1−N1 | 2.176(7) | Ag2−O1 | 2.273(7) | Ag2−N4 | 2.502(8) | Ag2−O4$^{iv}$ | 2.385(6) |
| Ag1−N6$^i$ | 2.193(7) | Ag2−N3 | 2.273(8) | | | | |
| N1−Ag1−N6$^i$ | 172.0(3) | O1−Ag2−N3 | 139.7(3) | O1−Ag2−N4 | 105.5(3) | O4$^{iv}$−Ag2−N4 | 92.5(2) |
| N3−Ag2−N4 | 90.7(3) | O1−Ag2−O4$^{iv}$ | 104.1(3) | N3−Ag2−O4$^{iv}$ | 111.9(3) | | |

Complex **4**

| | | | | | | | |
|---|---|---|---|---|---|---|---|
| Ag1−N2 | 2.299(4) | Ag1−O1W | 2.671(3) | Ag2−O3 | 2.536(3) | Ag2−N6$^i$ | 2.306(4) |
| Ag1−N5 | 2.304(4) | Ag2−N3$^{ii}$ | 2.369(4) | Ag2−O4 | 2.636(4) | Ag2−O1 | 2.471(3) |
| N2−Ag1−N5 | 137.91(14) | N3$^{ii}$−Ag2−O1 | 99.61(12) | N6$^i$−Ag2−O4 | 100.74(12) | O3−Ag2−O4 | 50.30(10) |
| N2−Ag1−O1 | 99.28(13) | N6$^i$−Ag2−O3 | 149.40(13) | N3$^{ii}$−Ag2−O4 | 105.82(13) | N6$^i$−Ag2−O1 | 113.20(12) |
| N5−Ag1−O1 | 120.75(12) | N3$^{ii}$−Ag2−O3 | 87.33(13) | O1−Ag2−O4 | 124.14(10) | N6$^i$−Ag2−N3$^{ii}$ | 113.60(13) |
| N2−Ag1−O1W | 88.99(12) | O1−Ag2−O3 | 82.99(11) | O1−Ag1−O1W | 125.47(12) | N5−Ag1−O1W | 78.61(12) |

Complex **5**

| | | | | | | | |
|---|---|---|---|---|---|---|---|
| Ag1−N5 | 2.238(5) | Ag1−O2 | 2.654(5) | Ag1−O1 | 2.617(5) | Ag1−N2 | 2.241(5) |
| N5−Ag1−N2 | 147.12(19) | N5−Ag1−O2 | 100.25(16) | O1−Ag1−O2 | 49.78(14) | N2−Ag1−O1 | 100.71(18) |
| N5−Ag1−O1 | 112.16(19) | N2−Ag1−O2 | 101.87(16) | | | | |

Complex **6**

| | | | | | | | |
|---|---|---|---|---|---|---|---|
| Ag1−O1 | 2.313(2) | Ag1−N2$^i$ | 2.454(3) | Ag1···Ag2$^{ii}$ | 3.1375(8) | | |
| O1−Ag1−O1$^i$ | 139.45(13) | N2$^i$−Ag1−N2 | 97.32(13) | O1$^i$−Ag1−N2$^i$ | 109.70(9) | O1−Ag1−N2$^i$ | 96.93(9) |

[a] Symmetry codes: (i) −x + 2, y, −z + $^1/_2$; (ii) −x + 2, −y + 1, −z; (iii) x, −y + 1, z + $^1/_2$; (v) −x + 1, −y + 1, −z. Symmetry codes: (i) x, y − 1, z; (ii) −x + 1, −y, −z + 2; (iii) −x + 1, −y, −z + 1; (vii) −x, −y, −z + 2. Symmetry codes: (i) x + 1, y, z; (ii) −x + 1, −y + 1, −z + 2; (iii) −x + 1, y + $^1/_2$, −z + $^3/_2$; (iv) x, −y + $^1/_2$, z + $^1/_2$. Symmetry codes: (i) −x + 1, −y + 1, −z; (ii) −x + 2, −y + 2, −z + 1. Symmetry code: (i) −x, −y + 1, −z + 1. Symmetry codes: (i) −x + 2, y, −z + $^1/_2$; (ii) −x + 2, −y + 2, −z; (v) −x + 1, y, −z + $^1/_2$; (vi) −x + 2, y, −z − $^1/_2$.

There are two Ag(I) ions, one mapym, half suc, and half H$_2$O in the asymmetric unit of **1**. Analysis of the local symmetry of the metal atoms and ligands shows that Ag1, Ag2, and the lattice water molecule reside on the crystallographic 2-fold axis (site occupancy factor (SOF) = $^1/_2$), whereas the suc locates on the inversion center. As depicted in Figure 1a, the Ag1 is located in a distorted tetrahedron geometry and coordinated by two symmetry-related mapym and suc ligands (Ag1−O2$^i$ = 2.240(2),

Ag1−N2$^{ii}$ = 2.453(3) Å). The distortion of the tetrahedron can be indicated by the calculated value of the $\tau_4$ parameter introduced by Houser[34] to describe the geometry of a four-coordinate metal system. Table 3 lists the $\tau_4$ parameter for all the four-coordinate Ag(I) ions in complex **1−6**. The $\tau_4$ values average 0.70, ranging from 0.58 to 0.79, showing the tetrahedral geometry is not perfect but distorted, where the distortion is in part due to the inherent lack of crystal field stabilization energy
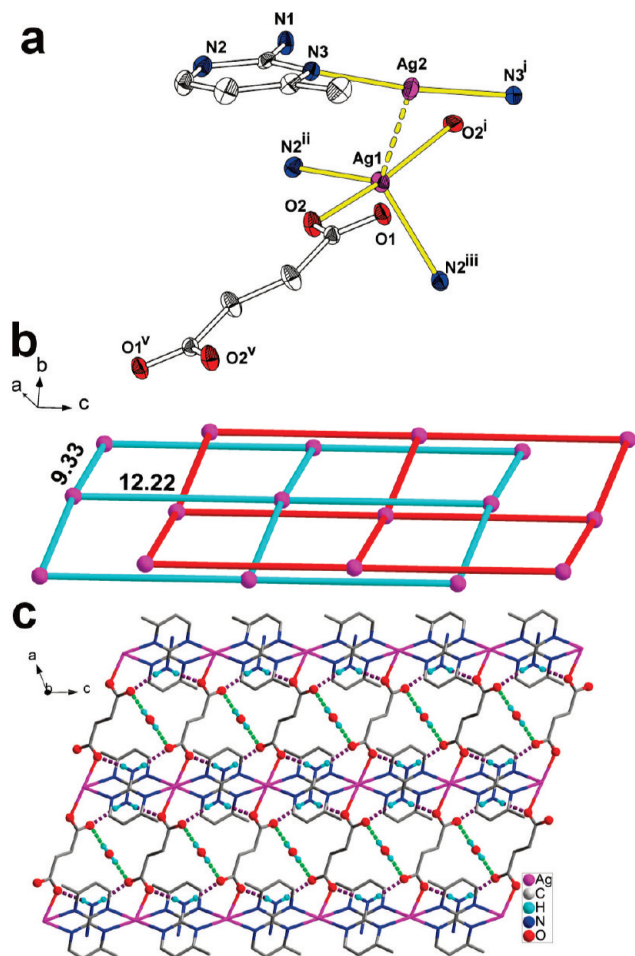
**Figure 1.** (a) Coordination environments of Ag(I) ions in **1** with the thermal ellipsoids at the 30% probability level. The lattice water molecule was omitted for clarity. Symmetry codes: (i) $-x + 2$, $y$, $-z + \frac{1}{2}$; (ii) $-x + 2$, $-y + 1$, $-z$; (iii) $x$, $-y + 1$, $z + \frac{1}{2}$; (v) $-x + 1$, $-y + 1$, $-z$. (b) Presentation of a pair of the interpenetrated $4^4$-sql net. (c) Scheme of a 2D sheet incorporating $O_{water}$—H$\cdots$O$_{suc}$ (green dashed lines) and N—H$\cdots$O$_{suc}$ (violet dashed lines) hydrogen bonds.

**Table 3. Four-Coordinate $\tau_4$ Parameters$^a$**

| silver | $\tau_4$ | $\alpha$ | $\beta$ |
|---|---|---|---|
| Ag1 in **1** | 0.58 | 166.50(15) | 111.23(15) |
| Ag1 in **2** | 0.68 | 144.05(12) | 120.08(13) |
| Ag2 in **3** | 0.77 | 139.7(3) | 111.9(3) |
| Ag1 in **4** | 0.69 | 137.91(14) | 125.47(12) |
| Ag1 in **5** | 0.71 | 147.12(19) | 112.16(19) |
| Ag1 in **6** | 0.79 | 139.45(13) | 109.70(9) |

$^a$ $\tau_4 = [360° - (\alpha + \beta)]/141°$, where $\alpha$ and $\beta$ are the largest angles around the metal centers. For a perfect square-planar geometry, $\tau_4$ equals 0, and a perfect tetrahedral geometry is described when $\tau_4$ equals 1.

that arises from a spherical $d^{10}$ electronic configuration.[35] The Ag2, coordinated by two symmetry-related N atoms from two different mapym ligands (Ag2—N3$^i$ = 2.167(3) Å), is located in an approximately linear environment with an angle of 170.49(16)°, which deviates from the ideal 180° due to the Ag$\cdots$O weak interaction (Ag2$\cdots$O1 = 2.814(3) Å). Both Ag—O and Ag—N bond lengths are well-matched to those observed in similar complexes.[36] It is worthy to note that the bond length of Ag1—N2 is obviously longer than that of Ag2—N3, which may be due to the crowded coordination environment around Ag1. The Ag$\cdots$Ag interaction also exists with a Ag1$\cdots$Ag2 separation of 3.0645(9) Å.

In **1**, the Ag(I) ions are linked by bidentate mapym to form 1D zigzag chains in which mapym is oppositely arranged, and the $\mu_2$-$\eta^1$:$\eta^0$:$\eta^1$:$\eta^0$ suc ligands extended the 1D chains into a single 2D slightly wavy net incorporating a window of 9.33 Å × 12.22 Å based on the Ag1$\cdots$Ag1 distances. The torsion angle (C6—C7—C7$^{ii}$—C6$^{ii}$ = 180.0°) about suc indicates the skeleton of suc does not twist.

To better understand the structure of **1**, the topological analysis approach is employed. In **1**, tetrahedral Ag1 ions as 4-connected joints are bridged by two kinds of 2-connected struts: mapym and suc ligand, so the 2D net can be simplified to be a wavy $4^4$-sql net which is interpenetrated by the neighboring one through a 2D → 2D parallel mode (Figure 1b), wherein one $4^4$-sql net shifts with respect to another one with a slippage of ca. 6.11 Å. The lattice water molecules are filled in the windows and hydrogen-bonded to carboxylic groups with the $O_{water}$—H$\cdots$O$_{suc}$ distance of 2.761(3) Å; moreover, the amino groups of mapym also interact with the carboxylic groups through N—H$\cdots$O$_{suc}$ hydrogen bonds with an average distance of 2.853(4) Å. Both of them reinforce the resultant 2D net (Figure 1c), which is further extended by nonclassical $C_{mapym}$—H$\cdots$O$_{water}$ hydrogen bonds into a 3D supramolecular framework (symmetry codes: (i) $-x + 2$, $y$, $-z + \frac{1}{2}$; (ii) $-x + 2$, $-y + 1$, $-z$).

**[Ag$_2$(mapym)$_2$(glu)·1.5H$_2$O]$_n$ (2).** The asymmetric unit of **2** consists of two crystallographically different Ag(I) ions, two mapym ligands, one glu, and one and a half lattice water molecules. As shown in Figure 2a, the Ag1 and Ag2 ions adopt tetrahedral and Y-shaped geometries, respectively. The $\tau_4$ parameter is 0.68 for Ag1, indicating a less distorted tetrahedron compared to that in complex **1**. The maximum angle and sum of angles around Ag2 are 152.32(13) and 352.60(13)°, respectively. The Ag—N and Ag—O bond lengths fall in the ranges 2.206(4)—2.236(3) and 2.298(3)—2.566(4) Å, respectively.

Similar to **1**, the Ag(I) ions in **2** are also linked by bidentate mapym to form 1D single zigzag chains in which the mapym are oppositely arranged. A pair of adjacent chains interconnect with each other through Ag$\cdots$Ag interaction (Ag1$\cdots$Ag2 = 3.1284(7) Å) to form a double-chain presented in Figure 2b. Alternatively, this double chain can also be considered as fused 10-membered macrocycles along the $c$-axis. Different from nontwisted suc in **1**, the glu ligands adopt a $\mu_3$-$\eta^1$:$\eta^1$:$\eta^1$:$\eta^0$ mode with a curled conformation (torsion of C11—C12—C13—C14 = 170.3(4)° and C15—C14—C13—C12 = 73.0(6)°) to extend the 1D chains into a 2D double-sheet incorporating a window of 12.46 Å × 10.04 Å on the basis of Ag1$\cdots$Ag1 distances (Figure 2c).

Amino groups are hydrogen bonded to carboxylic groups with an average N—H$\cdots$O$_{glu}$ distance of 2.935(5) Å. The lattice water molecules partially participate in stabilizing the 2D sheet through a $O_{water}$—H$\cdots$O$_{glu}$ hydrogen bond showing a distance of 2.822(10) Å. The C—H$\cdots\pi_{mapym}$ interaction [C5—H5A$\cdots$Cg1$^{vii}$: $d_{H\cdots Cg1}$ = 2.86 Å, $d_{C\cdots Cg1}$ = 3.591(6) Å, and $\theta$ = 134°; Cg1 is the centroid of aromatic ring N2/C1/N3/C2/C3/C4; $\theta$ is the angle of C—H$\cdots$Cg1, see Figure S1, Supporting Information] combines with the intersheet $O_{water}$—H$\cdots$O$_{glu}$ hydrogen bonds to stabilize the resultant 3D supramolecular framework (symmetry code: (vii) $-x$, $-y$, $-z + 2$).

**[Ag$_2$(mapym)$_2$(ipa)·2H$_2$O]$_n$ (3).** When using rigid H$_2$ipa, we obtained complex **3** as a 3D coordination polymer constructed through unusual 2D → 3D parallel interpenetration of deeply corrugated 2D $4^4$-sql nets. In the structure of **3**, as shown in Figure 3a, there are two crystallographically independent Ag(I) ions, two mapym, one ipa, as well as two
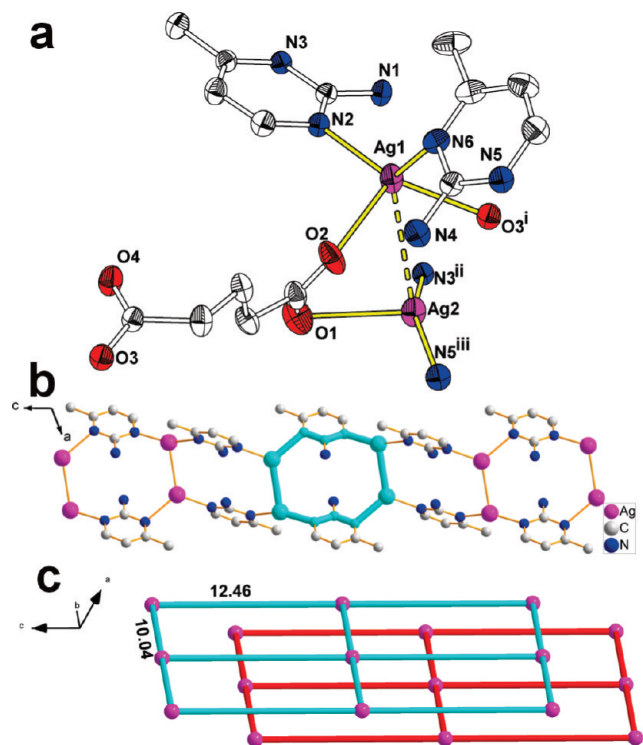
**Figure 2.** (a) Coordination environments of Ag(I) ions in **2** with the thermal ellipsoids at the 30% probability level. Lattice water molecules were omitted for clarity. Symmetry codes: (i) $x$, $y - 1$, $z$; (ii) $-x + 1$, $-y$, $-z + 2$; (iii) $-x + 1$, $-y$, $-z + 1$. (b) Scheme of the 1D double chain and the 10-membered macrocycle highlighted in cyan. (c) View of double $4^4$-sql nets.

solvent water molecules. Both Ag1 and Ag2 locate in the general positions. The Ag1 lies in a nearly linear geometry completed by two N atoms from two distinct mapym ligands ($\angle$N2—Ag1—N6$^i$ = 172.0(3)°). The Ag$\cdots$O weak interactions also exist around Ag1 (Ag1$\cdots$O3$^{iii}$ = 2.748(7), Ag1$\cdots$O1$^{ii}$ = 2.735(7) Å). The Ag2 is located in a distorted tetrahedron geometry and coordinated by two mapym and two ipa ligands with average Ag—O and Ag—N distances of 2.329(6) and 2.286(7) Å, respectively. The $\tau_4$ parameter is 0.77 for Ag2. Two mapym moieties bound to Ag1 in **3** form a dihedral angle of *ca.* 63°.

In **3**, the Ag(I) ions are fabricated by the bidentate mapym and $\mu_2$-$\eta^1$:$\eta^0$:$\eta^1$:$\eta^0$ ipa to form a 2D $4^4$-sql net (Figure 3b) incorporating 32-membered macrocycles. The size of the grid in the 2D net is 11.74 Å × 11.43 Å based on the Ag2$\cdots$Ag2 distances. This net exhibits a deeply corrugated character (Figure S2, Supporting Information) with a thickness of about 6.44 Å and a dihedral angle of 111.47°. As expected, the large dimensions and corrugated nature of the net allow them to interpenetrate in an extensive and unusual fashion. In **3**, as depicted in Figure 4a, each 2D $4^4$-sql net was simultaneously penetrated by the two neighboring ones ("upper" and "lower") to avoid large voids, and their mean planes are parallel and offset. In other words, as shown in Figure 4b, each window (blue) of the net is simultaneously catenated by the other two ones (yellow and red) and vice versa. Therefore, the 2D → 3D dimensional increase can also be regarded as being caused by the nets' polycatenation.

One lattice water molecule, one amino group, and two carboxylic groups are hydrogen-bonded to form a heteromeric $R_4^2(8)$ motif[37] (Figure S3, Supporting Information) with the average N—H$\cdots$O and O—H$\cdots$O distances of 2.949(10) and 2.872(17) Å, which combine with the $\pi\cdots\pi$
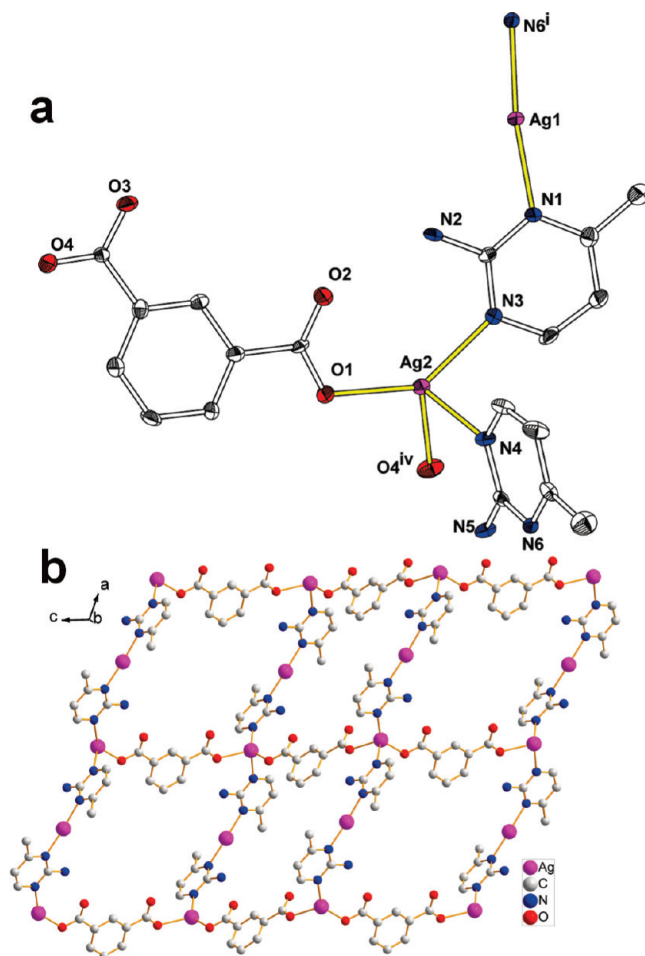


**Figure 3.** (a) ORTEP plot showing the coordination environments of Ag(I) ions in **3** with the thermal ellipsoids at the 30% probability level. Lattice water molecules were omitted for clarity. Symmetry codes: (i) $x + 1$, $y$, $z$; (iv) $x$, $-y + \frac{1}{2}$, $z + \frac{1}{2}$. (b) View of the undulated $4^4$-sql net in the structure of **3**.

interaction (centroid$\cdots$centroid = 3.636(6) Å; dihedral angle = 4.4(5)°, Figure S4, Supporting Information) and the C—H$\cdots\pi$ interactions (avg $d_{C\cdots Cg}$ = 3.621(12) Å; $\theta$ = 134°, Figure S5, Supporting Information) to enhance the stability of the resultant 3D framework.

**[Ag$_2$(mapym)$_2$(tpa)(H$_2$O)]$_n$ (4).** As shown in Figure 5a, in the asymmetric unit of **4**, there exist two Ag(I) ions, two mapym, two tpa and one coordinated water molecule. Both tpa ligands locates on the crystallographic inversion center with half occupancy. The coordination environments of Ag1 and Ag2 can be described as a distorted tetrahedron and a distorted square-pyramidal respectively. The tetrahedron is defined by two N atoms from two different mapym ligands and two O atoms from one tpa and one water molecule respectively (Ag1—O1$W$ = 2.671(3) and Ag1—N5 = 2.304(4) Å), and the $\tau_4$ parameter is 0.69 for Ag1. The square-pyramid is constructed by two N atoms from two different mapym ligands and three O atoms from two different tpa. Addison[38] also defined a geometric parameter $\tau_5$ ($\tau_5 = [(\theta - \varphi)/60]$, where $\theta$ and $\varphi$ are the angles between the donor atoms forming the basal plane in square-pyramidal geometry) to five-coordinate metal system as an index of the degree of distortion. The $\tau_5$ parameter for Ag2 is 0.42 (for ideal square-pyramidal geometry, $\tau_5 = 0$).

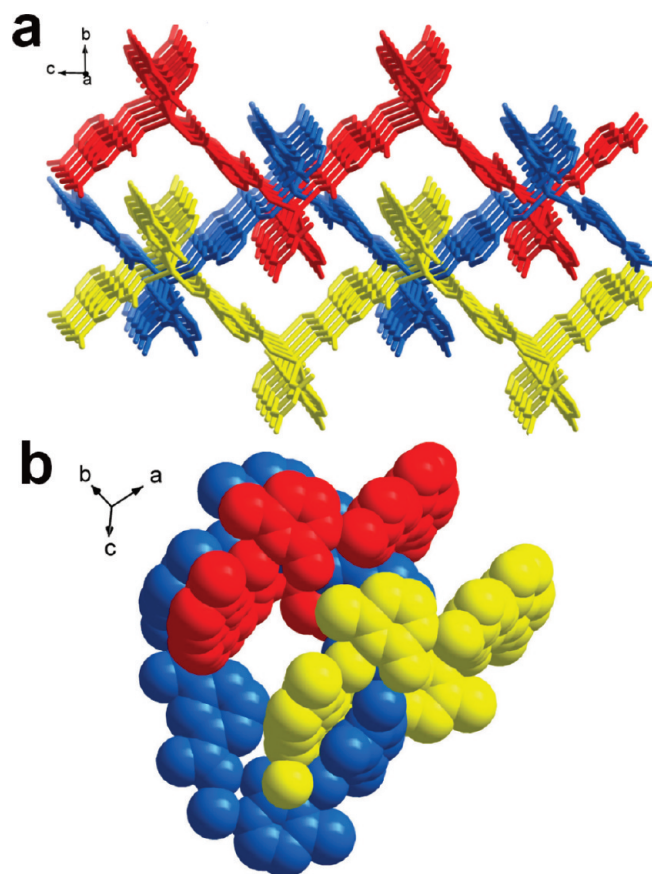Different from the 1D double chain in **2**, there is no Ag$\cdots$Ag interaction between adjacent 1D single chains in

**Figure 4.** (a) View of the 2D → 3D interpenetrating undulated $4^4$-sql net in the structure of **3**. (b) View of catenation of windows.
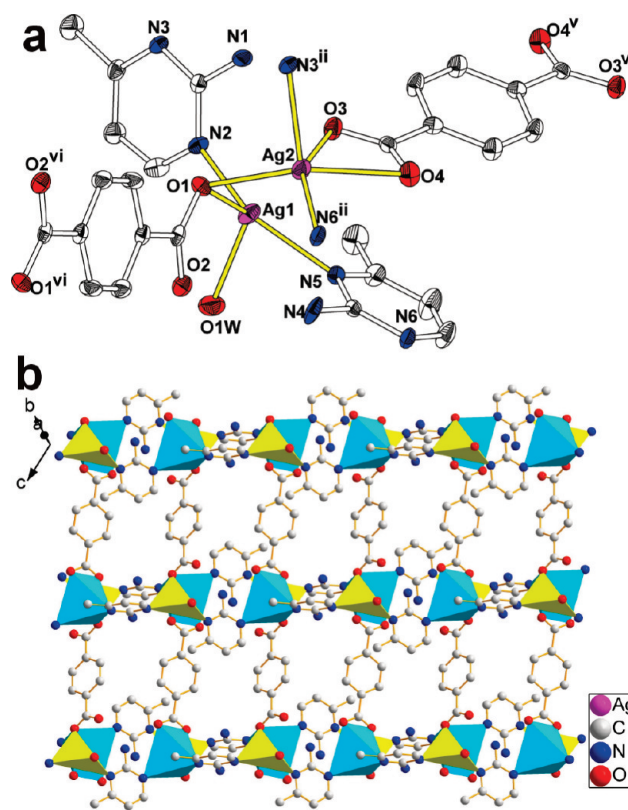


**Figure 5.** (a) ORTEP plot showing the coordination environments of Ag(I) ions in **4** with the thermal ellipsoids at the 30% probability level. The lattice water molecule was omitted for clarity. Symmetry codes: (ii) $-x + 2, -y + 2, -z + 1$; (v) $-x + 1, -y + 1, -z + 1$; (vi) $-x + 2, -y + 2, -z$. (b) View of the 2D net in the structure of **4** (yellow polyhedron, tetrahedron; cyan polyhedron, square-pyramid).

**4**, which is bridged by $\mu_2$-$\eta^2$:$\eta^0$ carboxylic groups of tpa into the resultant 1D double chain. Interestingly, the tpa ligands show two different coordination modes: $\mu_2$-$\eta^1$:$\eta^1$:$\eta^1$:$\eta^1$ chelating and $\mu_4$-$\eta^2$:$\eta^0$:$\eta^2$:$\eta^0$ bridging modes, which arrange alternately along the 1D double chains and extend them into the 2D net (Figure 5b), in which two kinds of coordinated carboxylic groups (C14 and C18) are almost coplanar with the central benzene ring, producing small dihedral angles between the individual groups and the benzene ring of 4.9(6) and 7.7(6)°, respectively.

The intrasheet N−H⋯$O_{tpa}$ hydrogen bonds consolidate the 2D sheet, whereas intersheet $O_{water}$−H⋯$O_{tpa}$ hydrogen bonds incorporate intrasheet N−H⋯$O_{tpa}$ hydrogen bonds to form a saddle-like heteromeric $R_4^2(8)$ motif. The adjacent 2D nets pack to form the supramolecular network through intersheet $O_{water}$−H⋯$O_{tpa}$ and C−H⋯$\pi$ ($d_{C⋯Cg}$ = 3.781(7) Å; $\theta$ = 144°, Figure S6, Supporting Information) interactions.

**[Ag(dmapym)$_2$(ox)$_{0.5}$·H$_2$O] (5).** As depicted in Figure 6a, complex **5** is a H-shaped discrete molecule and the asymmetric unit contains one Ag(I) ion, two dmapym, half ox, and one lattice water molecule. The Ag(I) ion is in a distorted tetrahedron geometry and coordinated by two N atoms from two different dmapym ligands and two O atoms from the same ox (avg Ag−N and Ag−O: 2.239(5) and 2.636(5) Å). The ox lying on the inversion center adopts the $\mu_2$-$\eta^1$:$\eta^1$:$\eta^1$:$\eta^1$ mode to bind two Ag(I) ions, forming a H-shaped molecule. The water molecules are hydrogen bonded to the Ag$_2$(dmapym)$_4$(ox) molecules to form the supramolecular 1D chain (Figure 6b) along the *a* axis containing $R_4^4(14)$ hydrogen bond motifs on the inversion center (O1W−H1WA⋯O2$^i$ = 2.741(6) and O1W−H1WB⋯O1$^{iv}$ = 2.775(6) Å).

Additionally, the dmapym adopts the monodentate coordination mode to bind the Ag(I) ions, which may be due to the steric effect of one more methyl group compared to mapym, so it does not extend the structure to the higher dimensionality. The self-complementary N−H⋯N hydrogen bonds involving stereochemically associative amino and hetero ring nitrogens form a $R_2^2(8)$ homomeric motif and combine with the $\pi$⋯$\pi$ (centroid⋯centroid = 3.856(4) Å; dihedral angle = 0°, Figure S7, Supporting Information) and C−H⋯$\pi$ (avg $d_{C⋯Cg}$ = 3.565(7) Å; $\theta$ = 135°, Figure S8) interactions to assemble the 1D chains into the resultant 3D supramolecular framework.

**[Ag(dmapym)(bbdc)$_{0.5}$·0.5H$_2$O]$_n$ (6).** X-ray analysis reveals that complex **6** crystallizes in a monoclinic system with space group $C2/c$. The asymmetric unit consists of two crystallographically independent Ag(I) ions, one dmapym, half bbdc, as well as half a solvent water molecule. A $C2$ axis passes through Ag1, Ag2, as well as the midpoint of C7−C7$^v$ bond of bbdc. The lattice water molecule is disordered related to the inversion center. As illustrated in Figure 7, the Ag1 and Ag2 locate in the distorted tetrahedral and linear geometries, respectively, without consideration of the Ag⋯Ag interaction. This tetrahedron is completed by two symmetry-related dmapym and bbdc ligands with Ag1−N2$^i$ and Ag1−O1 distances of 2.454(3) and 2.313(2) Å, respectively, and the $\tau_4$ parameter is 0.79 for Ag1, which indicate this tetrahedron is the least distorted one in complexes **1**−**6** (Table 3). The angle around Ag2 opens up to 160.07(11)°, which deviates from the ideal 180° due to the Ag⋯O weak interactions with Ag2⋯O1$^{ii}$ and
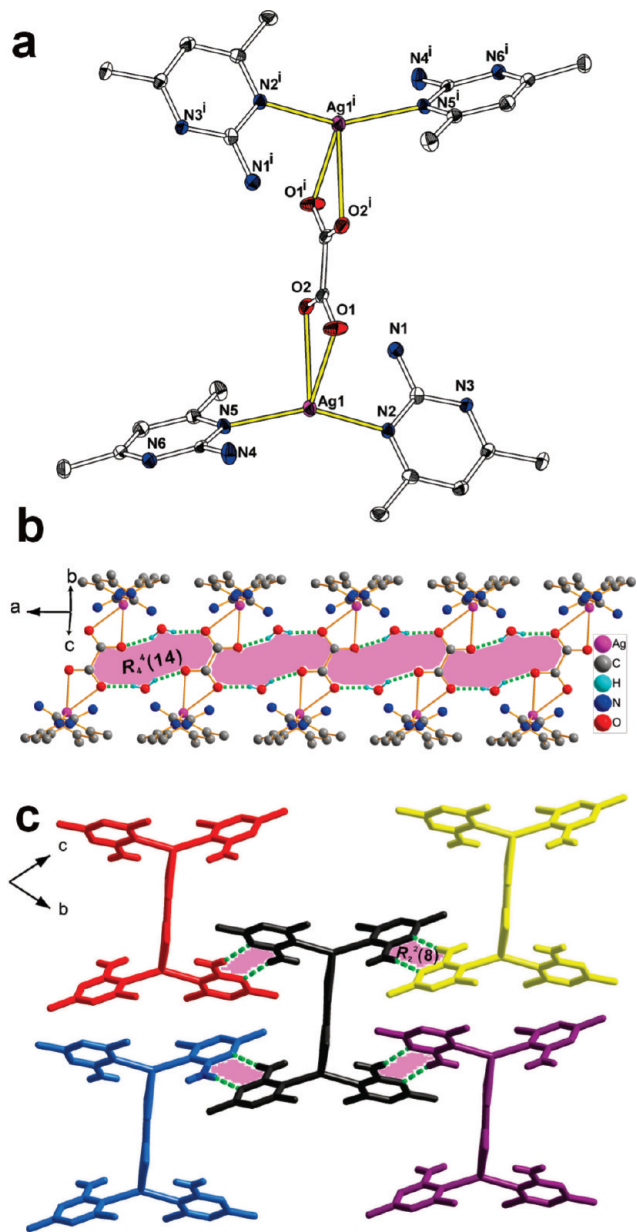
**a**

**b**

**c**

**Figure 6.** (a) Molecule structure of **5** with the thermal ellipsoids at 30% probability level. Lattice water molecule was omitted for clarity. Symmetry codes: (ii) $-x + 2, -y + 2, -z + 1$; (v) $-x + 1, -y + 1, -z + 1$; (vi) $-x + 2, -y + 2, -z$. (b) A view of the 1D supramolecular chain incorporating $R_4^4(14)$ hydrogen bond motifs. (c) The self-complementary N−H···N hydrogen bonds of two pyrimidine moieties with $R_2^2(8)$ motifs.

Ag2···O2[ii] distances of 3.188(3) and 2.776(3) Å, respectively (symmetry codes: (i) $-x + 2, y, -z + ^1/_2$; (ii) $-x + 2, -y + 2, -z$; (v) $-x + 1, y, -z + ^1/_2$).

The dmapym ligands act as $\mu_2$-bridges to link Ag(I) ions to form 1D single zigzag chains, and a pair of adjacent chains interconnect with each other to form a double-chain *via* Ag··· Ag interaction of 3.1284(7) Å, which is shorter than the van der Waals radii of Ag(I) (3.44 Å).[39] The $\mu_2$-$\eta^1$:$\eta^0$:$\eta^1$:$\eta^0$ bbdc ligands with a dihedral angle between two phenyl rings of 40.2(3)° extend the 1D chains into a double 4⁴-sql net incorporating a window of 12.10 Å × 15.68 Å on the basis of Ag1···Ag1 distances (Figure S9).

**Influence of Dicarboxylates and Substituents on Structures.**
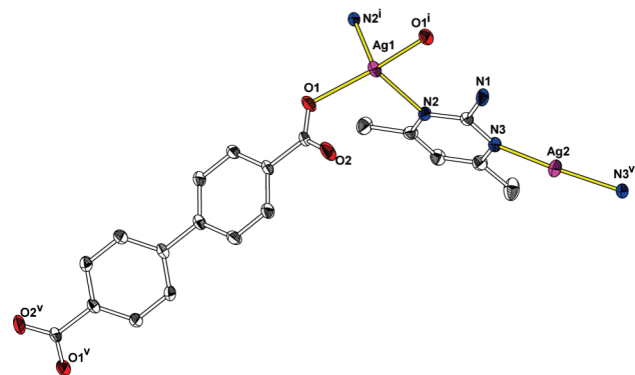It has been demonstrated that the structural diversities of



**Figure 7.** ORTEP plot showing the coordination environments of Ag(I) ions in **6** with the thermal ellipsoids at the 30% probability level. The lattice water molecule was omitted for clarity. Symmetry codes: (i) $-x + 2, y, -z + ^1/_2$; (v) $-x + 1, y, -z + ^1/_2$; (vi) $-x + 2, y, -z - ^1/_2$.

complexes **1−6** are undoubtedly related to the auxiliary ligands (configurations and coordination modes) and substituent effect (steric and electronic effects). The combined two factors are key points to influence the final complexes, which depends on the competition and adaptability of the components. That is to say, both kinds of organic ligands have to fine-tune themselves to satisfy the coordination preference of metal centers and the lower energetic arrangement in the assembly process.[40]

In six complexes, dicarboxylates varied in the assembly process are capable of diversifying the structures as well as coordination spheres of Ag(I). Four different coordination fashions [suc ($\mu_2$-$\eta^1$:$\eta^0$:$\eta^1$:$\eta^0$), glu ($\mu_3$-$\eta^1$:$\eta^1$:$\eta^1$:$\eta^0$), ipa ($\mu_2$-$\eta^1$:$\eta^0$:$\eta^1$:$\eta^0$), tpa ($\mu_4$-$\eta^2$:$\eta^0$:$\eta^2$:$\eta^0$ and $\mu_2$-$\eta^1$:$\eta^1$:$\eta^1$:$\eta^1$), ox ($\mu_2$-$\eta^1$:$\eta^1$:$\eta^1$:$\eta^1$), and bbdc ($\mu_2$-$\eta^1$:$\eta^0$:$\eta^1$:$\eta^0$)] have been observed in six dicarboxylate ligands (Scheme S1, Supporting Information). The suc, glu, ox, tpa, and bbdc act as linear (180°) rodlike spacers to give **1**, **2**, **4**, and **6** 2D 4⁴-sql nets incorporating different sizes and shapes of rectangle windows, whereas angular ipa (120°) favors formation of larger rings incorporating metal centers; as a result, the 2D → 3D parallel interpenetration framework is formed to avoid the large voids. Comparing complexes **5** and **6**, it seems reasonable to conclude that the increase of dimensionalities is caused by the competition between the steric and electronic effects of the methyl substituent. In detail, for **5**, the steric hindrance of the methyl groups overcomes the electronic effect and prevents Ag(I) ion from binding to the second N-coordination site on the pyrimidyl ring. In contrast to **5**, the electronic effect of methyl substituent in **6** dominates the assembly course and enhances the coordinative ability of the potential coordination site; consequently, a weak Ag−N bond ( > 2.4 Å) forms and the dimensionality increase from 0D to 2D is realized. The coordination spheres of Ag(I) in this work vary from linearity, trigon, tetrahedron, to square-pyramid, and they are also undoubtedly associated with the dicarboxylate-participated inclusion. In a word, different dicarboxylates and substituent effects are responsible for the structural diversity of the resultant coordination networks, in combination with the adaptable configuration of Ag(I) ion.

**IR Spectra.** The IR spectra (Figure S10, Supporting Information) of complexes **1−6** show features attributable to the carboxylic and amino group stretching vibrations. No band in the region 1690−1730 cm$^{-1}$ indicates complete deprotonation of the carboxylic groups. The characteristic bands of the carboxylic groups are shown in the range
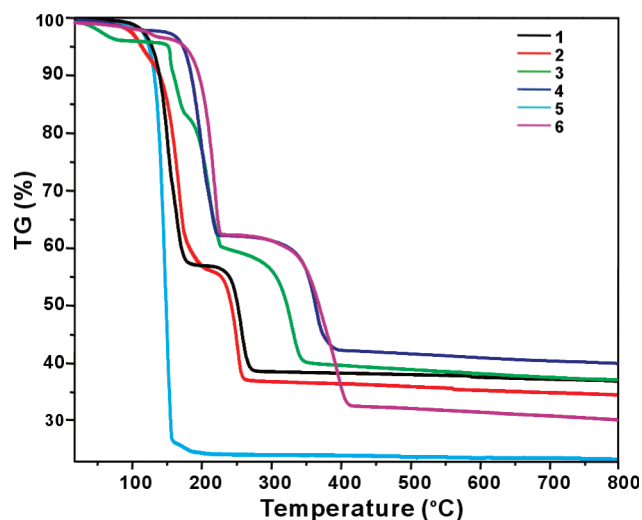
**Figure 8.** TGA curves for complexes **1**−**6**.

$1541-1665$ cm$^{-1}$ for asymmetric stretching and $1382-1482$ cm$^{-1}$ for symmetric stretching. Furthermore, the $(\nu_{as}-\nu_s)$ values are $181/180$ cm$^{-1}$ for **1**, $176/179$ cm$^{-1}$ for **2**, $178/112$ cm$^{-1}$ for **3**, $178/190$ cm$^{-1}$ for **4**, $195/209$ cm$^{-1}$ for **5**, and $124/148$ cm$^{-1}$ for **6**, respectively. The splitting of $\nu_{as}$(COO) indicates the different coordination modes of carboxylate,[41] being in agreement with their crystal structures. The N−H asymmetric and symmetric stretching bands fall in the ranges $3425-3325$ and $3175-3129$ cm$^{-1}$, respectively. This absorption is much sharper than O$_{water}$−H stretching and can, therefore, be differentiated.

**X-ray Power Diffraction Analyses and Thermal Analyses.** Powder X-ray diffraction (XRD) has been used to check the phase purity of the bulky samples in the solid state. For complexes **1**−**6**, the measured XRD patterns closely match the simulated patterns generated from the results of single-crystal diffraction data (Figure S11, Supporting Information), indicative of pure products. The thermogravimetric (TG) analysis was performed in N$_2$ atmosphere on polycrystalline samples of complexes **1**−**6**, and the TG curves are shown in Figure 8. The TG curve of **1** shows the first weight loss of 2.9% in the temperature range $25-118$ °C, which indicates the exclusion of lattice water molecules (calcd, 3.2%); with that, pyrolysis of the residual component occurs in two stages corresponding to the loss of mapym (obsd, 39.0%; calcd, 38.4%) and suc (obsd, 19.1%; calcd, 20.4%) ligands, respectively. For **2**, the loss of lattice water molecules (obsd, 4.2%; calcd, 4.6%), mapym (obsd, 37.8%; calcd, 36.9%), and glu (obsd, 22.0%; calcd, 21.1%) ligands happens in the ranges $25-113$, $114-203$, and $204-267$ °C, respectively. For **3**, an initial weight loss of 5.3% corresponds to the loss of solvent water (calcd, 5.7%). The second weight loss of 34.1% (calcd, 34.4%) corresponds to the loss of the mapym. The final weight loss of 25.4% corresponds to the loss of ipa (calcd, 25.9%). For **4**, the weight loss attributed to the gradual release of water molecules is observed in the range $25-153$ °C (obsd, 2.7%; calcd, 2.9%). The decomposition of residual composition occurs at 154 and 222 °C, corresponding to the loss of mapym (obsd, 34.9%; calcd, 35.4%) and tpa (obsd, 27.0%; calcd, 26.6%) ligands, respectively. For **5**, the curve shows one step decomposition in the temperature range $25-160$ °C and produces a 73.4% weight change, which corresponds to the loss of both solvent water molecules and organic ligands from the structure (calculated weight loss 74.0%). For **6**, the weight loss between 25 and 165 °C corresponds to the release
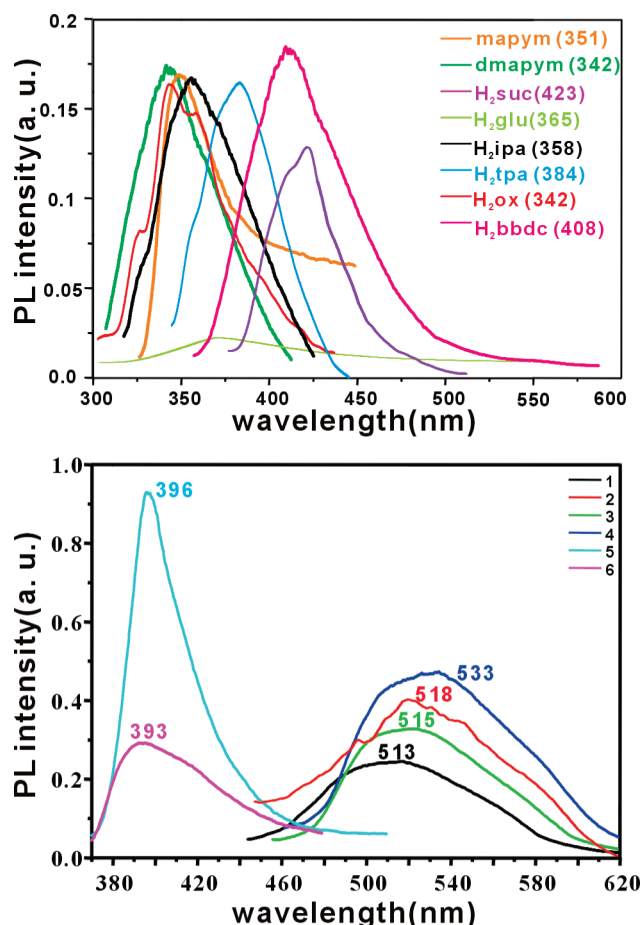




**Figure 9.** Photoluminescences of free ligands and complexes **1**−**6**.

of a water molecule (obsd, 2.2%; calcd, 2.5%). The removal of organic components occurs at two obvious stages: $165-232$ and $232-414$ °C, corresponding to the loss of mapym (obsd, 33.6%; calcd, 34.2%) and bbdc (obsd, 33.6%; calcd, 33.8%) ligands, respectively. Based on the analyzing TG curves of **1**−**4** and **6**, we find that the sequence of the ligands-release is the following: aminopyrimidyl ligands < dicarboxylate ligands, which indicates that the Ag−O bonds are more difficult to break than Ag−N bonds.[42] The exception happens in **5** with one step composition of organic ligands which may be due to the comparable strength of Ag−O and Ag−N bonds in **5**; consequently, the simultaneous bond breakage occurs during the heating process.

**Photoluminescence Properties.** The Ag(I) coordination complexes with aromatic ligands have received much attention for the development of hybrid photoluminescent materials.[43] Thus, solid-state photoluminescent properties of complexes **1**−**6** as well as free ligands were examined at room temperature. The photoluminescence spectra of the free ligands and complexes **1**−**6** are shown in Figure 9. The free ligands mapym, dmapym, H$_2$suc, H$_2$glu, H$_2$ipa, H$_2$tpa, H$_2$ox, and H$_2$bbdc display photoluminescence with emission maxima at 351, 342, 423, 365, 358, 384, 342, and 408 nm ($\lambda_{ex} = 300$ nm), respectively. It can be presumed that these peaks originate from the $\pi^* \rightarrow$ n or $\pi^* \rightarrow \pi$ transitions. To the best of our knowledge, the emission of dicarboxylate belongs to $\pi^* \rightarrow$ n transitions, which is very weak compared to that of the $\pi^* \rightarrow \pi$ transition of the mapym or dmapym, so the dicarboxylates almost have no contribution to the fluorescent emission of as-synthesized CCs.[44] Intense emissions are

observed at 513 nm for **1**, 518 nm for **2**, 515 nm for **3**, 533 nm for **4**, 396 nm for **5**, and 393 nm for **6**, respectively. When compared to the photoluminescence spectrum of the free mapym ligand, the emission bands of **1**−**4** are red-shifted by more than 150 nm, which may come from the electronic transition between p orbitals (filled orbitals) of coordinated N atoms and the 5s orbital (empty orbital) of Ag(I) ion, i.e., ligand-to-metal charge transfer (LMCT), mixed with metal-centered (d-s/d-p) transitions.[45] Different from **1**−**4**, obviously, the emissions of **5** and **6** are similar to that of dmapym and should be assigned to the intraligand transition of the coordinated N-donor ligand. The enhancement of luminescence of all complexes was attributed to ligand coordination to the metal center, which effectively increases the rigidity of the ligand and reduces the loss of energy by radiationless decay.[46]

## Conclusions

Six new CCs have been prepared by mixed aminopyrimidyl and dicarboxylate ligands under the ultrasonic treatment. They show diverse structures and dimensionalities from zero-dimensional discrete molecule (**5**), to two-dimensional sheets (**1**, **2**, **4**, and **6**), to 2D → 3D parallel interpenetrated three-dimensional strcuture (**3**). The changes of structure result from the various dicarboxylates and the adaptable coordination spheres of Ag(I). The substituent effects including steric and electronic effects also regulate the structures of resultant CCs. In addition, such CCs display modest thermal stability and strong solid-state fluorescent emission.

**Supporting Information Available:** Crystallographic data in CIF format, additional figures of the structures, hydrogen-bonding geometries, powder X-ray diffraction (PXRD) patterns, thermogravimetric analysis (TGA) curves, and IR spectra for **1**−**6**. This material is available free of charge via the Internet at http://pubs.acs.org.

## References

(1) (a) Batten, S. R.; Robson, R. *Angew. Chem., Int. Ed.* **1998**, *37*, 1460–1494. (b) Eddaoudi, M.; Moler, D. B.; Li, H.; Chen, B.; Reineke, T.; O'Keeffe, M.; Yaghi, O. M. *Acc. Chem. Res.* **2001**, *34*, 319–330. (c) Férey, G. *Chem. Soc. Rev.* **2008**, *37*, 191–214. (d) James, S. L. *Chem. Soc. Rev.* **2003**, *32*, 276–288. (e) Moulton, B.; Zaworotko, M. *J. Chem. Rev.* **2001**, *101*, 1629–1658. (f) Carlucci, L.; Ciani, G.; Proserpio, D. M. *Coord. Chem. Rev.* **2003**, *246*, 247–289. (g) Vittal, J. J. *Coord. Chem. Rev.* **2007**, *251*, 1781–1795. (h) Kitagawa, S.; Kitaura, R.; Noro, S. *Angew. Chem., Int. Ed.* **2004**, *43*, 2334–2375. (i) Zhang, J. P.; Huang, X. C.; Chen, X. M. *Chem. Soc. Rev.* **2009**, *38*, 2385–2396. (j) Zhang, J. P.; Chen, X. M. *J. Am. Chem. Soc.* **2008**, *130*, 6010–6017. (k) Zhao, B.; Chen, X. Y.; Cheng, P.; Liao, D. Z.; Yan, S. P.; Jiang, Z. H. *J. Am. Chem. Soc.* **2004**, *126*, 15394–15395. (l) Wu, D. Y.; Sato, O.; Einaga, Y.; Duan, C. Y. *Angew. Chem., Int. Ed.* **2009**, *48*, 1475–1478. (m) Wang, X. Y.; Wang, L.; Wang, Z. M.; Gao, S. *J. Am. Chem. Soc.* **2006**, *128*, 674–675. (n) Subramanian, S.; Zaworotko, M. J. *Angew. Chem., Int. Ed. Engl.* **1995**, *34*, 2127–2129. (o) Wang, M. S.; Guo, G. C.; Zou, W. Q.; Zhou, W. W.; Zhang, Z. J.; Xu, G.; Huang, J. S. *Angew. Chem., Int. Ed.* **2008**, *47*, 3565–3567. (p) Lan, A. J.; Li, K. H.; Wu, H. H.; Olson, D. H.; Emge, T. J.; Ki, W.; Hong, M. C.; Li, J. *Angew. Chem., Int. Ed.* **2009**, *48*, 2334–2338. (q) Zou, R.-Q.; Sakurai, H.; Han, S.; Zhong, R.-Q.; Xu, Q. *J. Am. Chem. Soc.* **2007**, *129*, 8402–8403. (r) Perry, J. J.; Perman, J. A.; Zaworotko, M. J. *Chem. Soc. Rev.* **2009**, *38*, 1400–1417. (s) Ward, M. D. *Science* **2003**, *300*, 1104–1105. (t) Kawamichi, T.; Haneda, T.; Kawano, M.; Fujita, M.

*Nature* **2009**, *461*, 633–635. (u) Zaworotko, M. J. *Nature* **2008**, *451*, 410–411. (v) Bu, X. H.; Tong, M. L.; Chang, H. C.; Kitagawa, S.; Batten, S. R. *Angew. Chem., Int. Ed.* **2004**, *43*, 192–195. (w) Hennigar, T. L.; Losier, P.; MacQuarrie, D. C.; Zaworotko, M. J.; Rogers, R. D. *Angew. Chem., Int. Ed. Engl.* **1997**, *36*, 972–973. (x) Moulton, B.; Zaworotko, M. *J. Chem. Rev.* **2001**, *101*, 1629–1658.

(2) (a) Roland, B. K.; Carter, C.; Zheng, Z. P. *J. Am. Chem. Soc.* **2002**, *124*, 6234–6235. (b) Lang, J. P.; Xu, Q. F.; Yuan, R. X.; Abrahams, B. F. *Angew. Chem., Int. Ed.* **2004**, *43*, 4741–4745. (c) Yang, J.; Ma, J. F.; Liu, Y. Y.; Ma, J. C.; Batten, S. R. *Inorg. Chem.* **2007**, *46*, 6542–6555. (d) Chiang, L. M.; Yeh, C. W.; Chan, Z. K.; Wang, K. M.; Chou, Y. C.; Chen, J. D.; Wang, J. C.; Lai, J. Y. *Cryst. Growth Des.* **2008**, *8*, 470–477. (e) Chen, H. C.; Hu, H. L.; Chan, Z. K.; Yeh, C. W.; Jia, H. W.; Wu, C. P.; Chen, J. D.; Wang, J. C. *Cryst. Growth. Des.* **2007**, *7*, 698–704.

(3) (a) Rispens, M. T.; Meetsma, A.; Rittberger, R.; Brabec, C. J.; Sariciftci, N. S.; Hummelen, J. C. *Chem. Commun.* **2003**, 2116–2118. (b) Zhang, W. H.; Song, Y. L.; Zhang, Y.; Lang, J. P. *Cryst. Growth Des.* **2008**, *8*, 253–258. (c) Chen, Y.; Li, H. X.; Liu, D.; Liu, L. L.; Li, N. Y.; Ye, H. Y.; Zhang, Y.; Lang, J. P. *Cryst. Growth Des.* **2008**, *8*, 3810–3816. (d) Tong, M. L.; Zheng, S. L.; Chen, X. M. *Chem.—Eur. J.* **2000**, *6*, 3729–3738.

(4) (a) Zheng, P. Q.; Ren, Y. P.; Long, L. S.; Huang, R. B.; Zheng, L. S. *Inorg. Chem.* **2005**, *44*, 1190–1192. (b) Wang, X. L.; Qin, C.; Wang, E. B.; Li, Y. G.; Su, Z. M.; Xu, L.; Carlucci, L. *Angew. Chem., Int. Ed.* **2005**, *44*, 5824–5827. (c) Yin, P. X.; Zhang, J.; Li, Z. J.; Qin, Y. Y.; Cheng, J. K.; Zhang, L.; Lin, Q. P.; Yao, Y. G. *Cryst. Growth Des.* **2009**, *9*, 4884–4896.

(5) (a) Forster, P. M.; Burbank, A. R.; Livage, C.; Férey, G.; Cheetham, A. K. *Chem. Commun.* **2004**, 368–369. (b) Huang, X. C.; Zhang, J. P.; Lin, Y. Y.; Yu, X. L.; Chen, X. M. *Chem. Commun.* **2004**, 1100–1101.

(6) (a) Kang, Y.; Lee, S. S.; Park, K. M.; Lee, S. H.; Kang, S. O.; Ko, J. *Inorg. Chem.* **2001**, *40*, 7027–7031. (b) Seo, J.; Song, M. R.; Sultana, K. F.; Kim, H. J.; Kim, J.; Lee, S. S. *J. Mol. Struct.* **2007**, *827*, 201–205. (c) Jung, O. S.; Kim, Y. J.; Lee, Y. A.; Park, K. M.; Lee, S. S. *Inorg. Chem.* **2003**, *42*, 844–850. (d) Yeh, C.-W.; Chen, T.-R.; Chen, J.-D.; Wang, J.-C. *Cryst. Growth. Des.* **2009**, *9*, 2595–2603. (e) Wang, Y.-H.; Chu, K.-L.; Chen, H.-C.; Yeh, C.-W.; Chan, Z.-K.; Suen, M.-C.; Chen, J.-D. *CrystEngComm* **2006**, *8*, 84–93. (f) Smith, G.; Cloutt, B. A.; Lynch, D. E.; Byriel, K. A.; Kennard, C. H. L. *Inorg. Chem.* **1998**, *37*, 3236–3242. (g) Ren, Y. P.; Kong, X. J.; Long, L. S.; Huang, R. B.; Zheng, L. S. *Cryst. Growth Des.* **2006**, *6*, 572–576.

(7) (a) Gural'skiy, I. A.; Escudero, D.; Frontera, A.; Solntsev, P. V.; Rusanov, E. B.; Chernega, A. N.; Krautscheid, H.; Domasevitch, K. V. *Dalton Trans.* **2009**, 2856–2864. (b) Domasevitch, K. V.; Solntsev, P. V.; Gural'skiy, I. A.; Krautscheid, H.; Rusanov, E. B.; Chernega, A. N.; Howard, J. A. K. *Dalton Trans.* **2007**, 3893–3905. (c) Schottel, B. L.; Chifotides, H. T.; Shatruk, M.; Chouai, A.; Pérez, L. M.; Bacsa, J.; Dunbar, K. R. *J. Am. Chem. Soc.* **2006**, *128*, 5895–5912.

(8) (a) Venkataraman, D.; Du, Y.; Wilson, S. R.; Hirsch, K.; Zhang, P.; Moore, J. S. *J. Chem. Educ.* **1997**, *74*, 915–919. (b) Cotton, F. A.; Wilkinson, G. *Advanced Inorganic Chemistry*, 5th ed.; Wiley: Chichester, 1988. (c) Cortez, S. M.; Raptis, R. G. *Coord. Chem. Rev.* **1998**, *169*, 363–426. (d) Sailaja, S.; Rajasekharan, M. V. *Inorg. Chem.* **2003**, *42*, 5675–5684. (e) Constable, E. C.; Housecroft, C. E.; Neuburger, M.; Poleschak, I.; Zehnder, M. *Polyhedron* **2003**, *22*, 93–108. (f) Liao, S.; Su, C.-Y.; Yeung, C.-H.; Xu, A.-W.; Zhang, H.-X.; Liu, H. Q. *Inorg. Chem. Commun.* **2000**, *3*, 405–408. (g) Burchell, T. J.; Eisler, D. J.; Puddephatt, R. J. *Cryst. Growth Des.* **2006**, *6*, 974–982. (h) Su, W.; Hong, M. *Angew. Chem., Int. Ed.* **2000**, *39*, 2911–2914. (i) Shimizu, G. K. H.; Enright, G. D. *Chem. Commun.* **1999**, 1485–1486. (j) John, F. C.; Fenske, D.; Power, W. P. *Angew. Chem., Int. Ed. Engl.* **1997**, *36*, 1176–1179. (k) Eduardo, J. F.; Concepción, G. M.; Laguna, A. *J. Am. Chem. Soc.* **2000**, *122*, 7287–7293. (l) Youngme, S.; Phuengphai, P.; Chaichit, N. *Inorg. Chim. Acta* **2005**, *358*, 849–853. (m) Navarro, J. A. R.; Salas, J. M.; Romero, M. A.; Faure, R. *J. Chem. Soc., Dalton Trans.* **1998**, 901–904. (n) Chen, C.-L.; Kang, B.-S.; Su, C.-Y. *Aust. J. Chem.* **2006**, *59*, 3–18. (o) Carlucci, L.; Ciani, G.; Proserpio, D. M.; Sironi, A. *Angew. Chem., Int. Ed. Engl.* **1995**, *34*, 1895–1898.

(9) (a) Che, C.-M.; Lai, S.-W. *Coord. Chem. Rev.* **2005**, *249*, 1296–1309. (b) Phillips, D. L.; Che, C.-M.; Leung, K.-H.; Mao, Z.; Tse, M.-C. *Coord. Chem. Rev.* **2005**, *249*, 1476–1490.

(10) (a) Fenske, D.; Persau, C.; Dehnen, S.; Anson, C. E. *Angew. Chem., Int. Ed.* **2004**, *43*, 305–309. (b) Chitsaz, S.; Fenske, D.; Fuhr, O. *Angew. Chem. Int. Ed.* **2006**, *45*, 8055–8059. (c) Anson, C. E.; Eichhöfer, A.; Issac, I.; Fenske, D.; Fuhr, O.; Sevillano, P.; Persau, C.; Stalke, D.; Zhang, J. T. *Angew. Chem., Int. Ed.* **2008**, *47*, 1326–1331.

(11) Luo, T. T.; Liu, Y. H.; Chan, C. C.; Huang, S. M.; Chang, B. C.; Lu, Y. L.; Lee, G. H.; Peng, S. M.; Wang, J. C.; Lu, K. L. *Inorg. Chem.* **2007**, *46*, 10044–10046. (b) Zheng, X. D.; Jiang, L.; Feng, X. L.; Lu, T. B. *Inorg. Chem.* **2008**, *47*, 10858–10865. (c) Khlobystov, A. N.; Blake, A. J.; Champness, N. R.; Lemenovskii, D. A.; Majouga, A. G.; Zyk, N. V.; Schröder, M. *Coord. Chem. Rev.* **2001**, *222*, 155–192. (d) Deng, Z. P.; Zhu, L. N.; Gao, S.; Huo, L. H.; Ng, S. W. *Cryst. Growth Des.* **2008**, *8*, 3277–3284. (e) Han, L.; Hong, M. C. *Inorg. Chem. Commun.* **2005**, *8*, 406–419. (f) Bowyer, P. K.; Porter, K. A.; Rae, A. D.; Willis, A. C.; Wild, S. B. *Chem. Commun.* **1998**, 1153–1154.

(12) (a) Huang, X. C.; Zhang, J. P.; Chen, X. M. *Cryst. Growth Des.* **2006**, *6*, 1194–1198. (b) Huang, G.; Tsang, C. K.; Xu, Z.; Li, K.; Zeller, M.; Hunter, A. D.; Chui, S. S. Y.; Che, C. M. *Cryst. Growth Des.* **2009**, *9*, 1444–1451. (c) Sun, D.; Luo, G. G.; Xu, Q. J.; Zhang, N.; Jin, Y. C.; Zhao, H. X.; Lin, L. R.; Huang, R. B.; Zheng, L. S. *Inorg. Chem. Commun.* **2009**, *12*, 782–784.

(13) (a) Cordes, D. B.; Hanton, L. R. *Inorg. Chem.* **2007**, *46*, 1634–1644. (b) Black, C. A.; Hanton, L. R. *Cryst. Growth. Des.* **2007**, *7*, 1868–1871. (c) Zhang, J.; Chen, Y.-B.; Chen, S.-M.; Li, Z.-J.; Cheng, J.-K.; Yao, Y.-G. *Inorg. Chem.* **2006**, *45*, 3161–3163. (d) Blake, A. J.; Champness, N. R.; Cooke, P. A.; Nicolson, J. E. B. *Chem. Commun.* **2000**, 665–666. (e) MacGillivray, L. R.; Subramanain, S.; Zaworotko, M. J. *J. Chem. Soc., Chem. Commun.* **1994**, 1325–1326.

(14) (a) Lu, X. Q.; Qiao, Y .Q.; He, J. R.; Pan, M.; Kang, B. S.; Su, C. Y. *Cryst. Growth Des.* **2006**, *6*, 1910–1914. (b) Argent, S. P.; Adams, H.; Riis-Johannessen, T.; Jeffery, J. C.; Harding, L. P.; Clegg, W.; Harringtond, R. W.; Ward, M. D. *Dalton Trans.* **2006**, 4996–5013.

(15) (a) Zhang, J. P.; Kitagawa, S. *J. Am. Chem. Soc.* **2008**, *130*, 907–917. (b) Ni, Z.; Vittal, J. J. *Cryst. Growth Des.* **2001**, *1*, 195–197. (c) Dong, Y.-B.; Wang, P.; Huang, R.-Q.; Smith, M. D. *Inorg. Chem.* **2004**, *43*, 4727–4739. (d) Liu, F.-Q.; Tilley, T. D. *Inorg. Chem.* **1997**, *36*, 5090–5096. (e) Banfi, S.; Carlucci, L.; Caruso, E.; Ciani, G.; Proserpio, D. M. *Cryst. Growth Des.* **2004**, *4*, 29–32. (f) Hoskins, B. F.; Robson, R.; Slizys, D. A. *J. Am. Chem. Soc.* **1997**, *119*, 2952–2953. (g) Kuang, X.; Wu, X; Yu, R.; Donahue, J. P.; Huang, J.; Lu, C. Z. *Nature Chem.* **2010**, *2*, 461–465.

(16) Jin, C. M.; Wu, L. Y.; Lu, H.; Xu, Y. *Cryst. Growth. Des.* **2008**, *6*, 215–218.

(17) (a) Chu, Q.; Liu, G. X.; Huang, Y. Q.; Wang, X. F.; Sun, W. Y. *Dalton Trans.* **2007**, 4302–4311. (b) Zang, S. Q.; Su, Y.; Duan, C. Y.; Li, Y. Z.; Zhu, H. Z.; Meng, Q. J. *Chem. Commun.* **2006**, 4997–4999. (c) Fang, Q. R.; Zhu, G. S.; Xue, M.; Sun, J. Y.; Sun, F. X.; Qiu, S. L. *Inorg. Chem.* **2006**, *45*, 3582–3587. (d) Li, H.; Eddaoudi, M.; O'Keeffe, M.; Yaghi, O. M. *Nature* **1999**, *402*, 276–279. (e) Deng, H.; Doonan, C. J.; Furukawa, H.; Ferreira, R. B.; Towne, J.; Knobler, C. B.; Wang, B.; Yaghi, O. M. *Science* **2010**, *327*, 846–850.

(18) (a) Michaelides, A.; Kiritsis, V.; Skoulika, S.; Aubry, A. *Angew. Chem., Int. Ed. Engl.* **1993**, *32*, 1495–1497. (b) Li, F.; Li, T.; Yuan, D.; Lv, J.; Cao, R. *Inorg. Chem. Commun.* **2006**, *9*, 691–694. (c) Long, J. R.; Yaghi, O. M. *Chem. Soc. Rev.* **2009**, *38*, 1213–1214.

(19) (a) Zhou, Y. F.; Zhao, Y. J.; Sun, D. F.; Weng, J. B.; Cao, R.; Hong, M. C. *Polyhedron* **2003**, *22*, 1231–1235. (b) Zhang, L. Y.; Liu, G. F.; Zheng, S. L.; Ye, B. H.; Zhang, X. M.; Chen, X. M. *Eur. J. Inorg. Chem.* **2003**, 2965–2971. (c) Chen, X. M.; Liu, G. F. *Chem.—Eur. J.* **2002**, *8*, 4811–4817.

(20) (a) Zhang, X. M.; Tong, M. L.; Chen, X. M. *Angew. Chem., Int. Ed.* **2002**, *41*, 1029–1031. (b) Sun, D. F.; Cao, R.; Liang, Y. C.; Shi, Q.; Su, W. P.; Hong, M. C. *J. Chem. Soc., Dalton Trans.* **2001**, 2335–2340. (c) Sun, D.; Xu, Q. J.; Ma, C. Y.; Zhang, N.; Huang, R. B.; Zheng, L. S. *CrystEngComm*, **2010**, http://dx.doi.org/10.1039/C0CE00017E. (d) Hogben, T.; Douthwaite, R. E.; Gillie, L. J.; Whitwood, A. C. *CrystEngComm* **2006**, *8*, 866–868.

(21) (a) Krizanovic, O.; Sabat, M.; Beyerle-Pfnür, R.; Lippert, B. *J. Am. Chem. Soc.* **1993**, *115*, 5538–5548. (b) Lin, C.-Y.; Chan, Z.-K.; Yeh, C.-W.; Wu, C.-J.; Chen, J.-D.; Wang, J.-C. *CrystEngComm* **2006**, *8*, 841–846. (c) Wang, Y.-H.; Chu, K.-L.; Chen, H.-C.; Yeh, C.-W.; Chan, Z.-K.; Suen, M.-C.; Chen, J.-D. *CrystEngComm* **2006**, *8*, 84–93.

(22) (a) Shen, W. Z.; Costisella, B.; Lippert, B. *J. Chem. Soc., Dalton Trans.* **2007**, 851–858. (b) Navarro, J. A. R.; Barea, E.; Galindo, M. A.; Salas, J. M.; Romero, M. A.; Quirós, M.; Masciocchi, N.; Galli, S.; Sironi, A.; Lippert, B. *J. Solid State Chem.* **2005**, *178*, 2436–2451.

(23) Marzilli, L. G.; Summers, M. F.; Zangrando, E.; Bresciani-Pahor, N.; Randaccio, L. *J. Am. Chem. Soc.* **1986**, *108*, 4830–4838.

(24) (a) Spannenberg, A.; Arndt, P.; Kempe, R. *Angew. Chem., Int. Ed.* **1998**, *37*, 832–835. (b) Kempe, R.; Arndt, P. *Inorg. Chem.* **1996**, *35*, 2644–2646. (c) Cotton, F. A.; Yokochi, A. *Inorg. Chem.* **1998**, *37*, 2723–2728. (d) Li, Y.; Han, B.; Kadish, K. M.; Bear, J. L. *Inorg. Chem.*

**1993**, *32*, 4175–4175. (e) Bear, J. L.; Yao, C.-L.; Capdevielle, F. J.; Kadish, K. M. *Inorg. Chem.* **1988**, *27*, 3782–3785.

(25) (a) Lin, C.-Y.; Chan, Z.-K.; Yeh, C.-W.; Wu, C.-J.; Chen, J.-D.; Wang, J.-C. *CrystEngComm* **2006**, *8*, 841–846. (b) Wang, Y.-H.; Chu, K.-L.; Chen, H.-C.; Yeh, C.-W.; Chan, Z.-K.; Suen, M.-C.; Chen, J.-D. *CrystEngComm* **2006**, *8*, 84–93. (c) Domasevitch, K. V.; Boldog, I.; Rusanov, E. B.; Hunger, J.; Blaurock, S.; Schröder, M.; Sieler, J. *Z. Anorg. Allg. Chem.* **2005**, *631*, 1095–1100.

(26) (a) Sun, D.; Luo, G. G.; Zhang, N.; Chen, J. H.; Huang, R. B.; Lin, L. R.; Zheng, L. S. *Polyhedron* **2009**, *28*, 2983–2988. (b) Sun, D.; Luo, G. G.; Zhang, N.; Xu, Q. J.; Yang, C. F.; Wei, Z. H.; Jin, Y. C.; Lin, L. R.; Huang, R. B.; Zheng, L. S. *Inorg. Chem. Commun.* **2010**, *13*, 290–293. (c) Sun, D.; Zhang, N.; Xu, Q. J.; Luo, G. G.; Huang, R. B.; Zheng, L. S. *J. Mol. Struct.* **2010**, *969*, 176–181. (d) Sun, D.; Zhang, N.; Xu, Q. J.; Luo, G. G.; Huang, R. B.; Zheng, L. S. *J. Mol. Struct.* **2010**, *970*, 134–138. (e) Sun, D.; Luo, G. G.; Zhang, N.; Xu, Q. J.; Jin, Y. C.; Wei, Z. H.; Yang, C. F.; Lin, L. R.; Huang, R. B.; Zheng, L. S. *Inorg. Chem. Commun.* **2010**, *13*, 306–309. (f) Sun, D.; Luo, G. G.; Zhang, N.; Xu, Q. J.; Huang, R. B.; Zheng, L. S. *Polyhedron* **2010**, *29*, 1243–1250. (g) Sun, D.; Luo, G. G.; Zhang, N.; Xu, Q. J.; Wei, Z. H.; Yang, C. F.; Lin, L. R.; Huang, R. B.; Zheng, L. S. *Bull. Chem. Soc. Jpn.* **2010**, *83*, 173–175. (h) Sun, D.; Luo, G. G.; Zhang, N.; Wei, Z. H.; Yang, C. F.; Huang, R. B.; Zheng, L. S. *Chem. Lett.* **2010**, *39*, 190–191.

(27) Higashi, T. *ABSCOR, Empirical Absorption Correction based on Fourier Series Approximation*; Rigaku Corporation: Tokyo, 1995.

(28) Sheldrick, G. M. *SHELXS-97, Program for X-ray Crystal Structure Determination*; University of Gottingen: Germany, 1997.

(29) Sheldrick, G. M. *SHELXL-97, Program for X-ray Crystal Structure Refinement*; University of Gottingen: Germany, 1997.

(30) Spek, A. L. *Implemented as the PLATON Procedure, a Multipurpose Crystallographic Tool*; Utrecht University,: Utrecht, The Netherlands, 1998.

(31) Sun, D. F.; Cao, R.; Bi, W. H.; Hong, M. C.; Chang, Y. L. *Inorg. Chim. Acta* **2004**, *357*, 991.

(32) Sun, D.; Luo, G. G.; Zhang, N.; Wei, Z. H.; Yang, C. F.; Xu, Q. J.; Huang, R. B.; Zheng, L. S. *Chem. Lett.* **2010**, *39*, 190.

(33) (a) Suslick, K. S.; Price, G. *Annu. Rev. Mater. Sci.* **1999**, *29*, 295–326. (b) McNamara, W. B., III; Didenko, Y.; Suslick, K. S. *Nature* **1999**, *401*, 772–775. (c) Flannigan, D. J.; Suslick, K. S. *Nature* **2005**, *434*, 52–55. (d) Bang, J. H.; Suslick, K. S. *J. Am. Chem. Soc.* **2007**, *129*, 2242–2243. (e) Dhas, N. A.; Suslick, K. S. *J. Am. Chem. Soc.* **2005**, *127*, 2368–2369. (f) Skrabalak, S. E.; Suslick, K. S. *J. Am. Chem. Soc.* **2005**, *127*, 9990–9991. (g) Suh, W. H.; Suslick, K. S. *J. Am. Chem. Soc.* **2005**, *127*, 12007–12010. (h) Didenko, Y. T.; Suslick, K. S. *J. Am. Chem. Soc.* **2005**, *127*, 12196–12197.

(34) Yang, L.; Powell, D. R.; Houser, R. P. *Dalton Trans.* **2007**, 955–964.

(35) (a) Côté, A. P.; Shimizu, G. K. H. *Coord. Chem. Rev.* **2003**, *245*, 49–64. (b) Munakata, M.; Wu, L. P.; Kuroda-Sowa, T. *Adv. Inorg. Chem.* **1999**, *46*, 173–303.

(36) (a) Sun, D.; Zhang, N.; Xu, Q. J.; Huang, R. B.; Zheng, L. S. *J. Organomet. Chem.* **2010**, *695*, 1598–1602. (b) Sun, D.; Zhang, N.; Luo, G. G.; Xu, Q. J.; Huang, R. B.; Zheng, L. S. *Polyhedron* **2010**, *29*, 1842–1848. (c) Degtyarenko, A. S.; Solntsev, P. V.; Krautscheid, H.; Rusanov, E. B.; Chernega, A. N.; Domasevitch, K. V. *New J. Chem.* **2008**, *32*, 1910–1918. (d) Gural'skiy, I. A.; Solntsev, P. V.; Krautscheid, H.; Domasevitch, K. V. *Chem. Commun.* **2006**, 4808–4810. (e) Katagiri, K.; Ikeda, T.; Tominaga, M.; Masu, H.; Azumaya, I. *Cryst. Growth. Des.* **2010**, http://dx.doi.org/10.1021/cg100013g. (f) Kong, X. J.; Ren, Y. P.; Zheng, P. Q.; Long, Y. X.; Long, L. S.; Huang, R. B.; Zheng, L. S. *Inorg. Chem.* **2006**, *45*, 10702–10711.

(37) Bernstein, J.; Davis, R. E.; Shimoni, L.; Chang, N.-L. *Angew. Chem., Int. Ed. Engl.* **1995**, *34*, 1555–1573.

(38) Addison, A. W.; Rao, T. N.; Reedijk, J.; van Rijn, J.; Verschoor, G. C. *J. Chem. Soc., Dalton Trans.* **1984**, 1349–1356.

(39) (a) Pyykkö, P. *Chem. Rev.* **1997**, *97*, 597–636. (b) Jansen, M. *Angew. Chem., Int. Ed.* **1987**, *26*, 1098–1110. (c) Liu, D.; Li, H. X.; Ren, Z. G.; Chen, Y.; Zhang, Y.; Lang, J. P. *Cryst. Growth Des.* **2009**, *9*, 4562–4566.

(40) Wang, S.-N.; Bai, J.; Li, Y.-Z.; Pan, Y.; Scheerb, M.; You, X.-Z. *CrystEngComm* **2007**, *9*, 1084–1095.

(41) (a) Nakamoto, K. *Infrared and Raman Spectra of Inorganic and Coordination Compounds*; John Wiley & Sons: New York, 1986. (b) Deacon, G. B.; Phillips, R. J. *Coord. Chem. Rev.* **1980**, *33*, 227–250.

(42) Zhao, X. F.; Zhu, L. G. *Cryst. Growth Des.* **2009**, *9*, 4407–4414.

(43) (a) Yam, V. W. W.; Lo, K. K. W. *Chem. Soc. Rev.* **1999**, *28*, 323–334. (b) Allendorf, M. D.; Bauer, C. A.; Bhakta, R. K.; Houk, R. J. T. *Chem. Soc. Rev.* **2009**, *38*, 1330–1352. (c) Wu, C.-D.; Ngo, H. L.; Lin,

W. *Chem. Commun.* **2004**, 1588–1589. (d) Chan, S. C.; Chan, M. C. W.; Wang, Y.; Che, C. M.; Cheung, K. K.; Zhu, N. *Chem.−Eur. J.* **2001**, *7*, 4180–4190. (e) Che, C. M.; Tse, M. C.; Chan, M. C. W.; Cheung, K. K.; Phillips, D. L.; Leung, K. H. *J. Am. Chem. Soc.* **2000**, *122*, 2464–2468.

(44) Chen, W. J.; Wang, Y.; Chen, C.; Yue, Q.; Yuan, H. M.; Chen, J. S.; Wang, S. N. *Inorg. Chem.* **2003**, *42*, 944–946.
(45) Yam. V. W. W. *Acc. Chem. Res.* **2002**, *35*, 555–563.
(46) Yi, L.; Zhu, L.-N.; Ding, B.; Cheng, P.; Liao, D.-Z.; Yan, S.-P.; Jiang, Z.-H. *Inorg. Chem. Commun.* **2003**, *6*, 1209–1212.